Quantitative rates of *in vivo* bone generation for Bioglass® and hydroxyapatite particles as bone graft substitute

Y. FUJISHIRO, L. L. HENCH
Department of Materials, Imperial College of Science, Technology and Medicine, Prince Consort Road, London SW7 2BP, UK
H. OONISHI
Department of Orthopaedic Surgery, Artificial Joint Section and Biomaterials Research Laboratory, Osaka-Minami National Hospital, Kido-Cho, Kawachinagano-Shi, Osaka 586, Japan

Rates of *in vivo* bone generation were characterized by point-counting analysis of particulate Bioglass® and synthetic hydroxyapatite (HA) in rabbit femora. New bony tissue was observed in $\sim 20\%$ of the image area around Bioglass® particles at 1 wk, and the degree of trabecular bone growth increased with time. The interparticle space of Bioglass® was filled by 80% bonding bone between 6 and 12 wk. The rate constants of trabecular bone growth in the presence of Bioglass® were $\sim 10.9 \times 10^{-3}\,d^{-1}$ at the periphery of the implantation site. HA particles led to smaller rate constants of $\sim 4.6 \times 10^{-3}\,d^{-1}$ at the periphery, and the HA particles developed very small amounts of bridging bone. The quantitative rate of bone growth matched well with previously measured bioactive indices of the materials.

1. Introduction

Biocompatible materials, such as calcium phosphates (α-tetracalcium phosphate (TCP), hydroxyapatite (HA) etc.) and bioactive glasses can be effective in the repair of bone defects during orthopaedic surgery. These materials have been found by observation to exhibit varying degrees of osteoconductive behaviour. The 45S5 bioactive glass (Bioglass®) is known as a highly bioactive glass particulate, and has been in clinical use for filling bone cavities and replacement of lost bone [1, 2]. The bone response to Bioglass® was compared by our group with α-TCP, β-TCP, Tetracalcium phosphate (TeCP), octacalciumphosphate (Ocp), and synthetic HA using a rabbit femoral defect model [3, 4]. Bioglass® was shown to induce the formation of trabecular bone in some areas between 2 and 7 d, and extensive bone bridges were formed at longer times [3, 4]. The area of new bone around the HA particles was low, even for 12 wk; many non-bone cavities were observed [3, 4]. These results clearly illustrate the difference in *in vivo* response between Bioglass® particles and HA particles. However, quantitative analysis of *in vivo* bone generation is important for establishing the mechanism and the properties of alloplastic implant materials [5]. Thus, quantitative analysis of *in vivo* bone growth, the amounts of implanted Bioglass® and HAp particles, regenerated bone, and soft tissue regions, were determined by a point-counting analysis of scanning electron micrographs (SEM) of sections from implanted samples in rabbit [3, 4]. The effects of materials and observation locations, are considered with respect to the calculated rates of bone generation.

2. Experimental procedure

The samples of 45S5 bioactive glass® (45% SiO_2, 24.5% Na_2O, 24.5% CaO, 6% P_2O_5 wt%) or synthetic HA particles, were separated to a size range of 100–300 μm, implanted into rabbit femora for 5 d to 12 wk. Experimental details are given elsewhere [3, 4]. The bone-implant samples were observed via back-scattered SEM analysis.

All data from micrographs were measured by hand-point-counting using a 5 mm square grid sheet ($24 \times 30 = 720$ points/image). Micrographs of different magnifications were used for counting.

The unit volumes of particle N_p, new bone, N_b, original bone, N_{ob}, and soft tissue, N_{nb}, were estimated by percentage of points, respectively [6]

$$N_i(\%) = P_i/P_{total} \times 100 \quad (1)$$

The ratio of bone growth, x, is calculated from

$$N_{space}(\%) = 100 - (N_p + N_{ob}) \quad (2)$$

$$x = N_b/N_{space} \quad (3)$$

where N_{space} is the percentage of interparticle space around Bioglass® or HA particles.

0957–4530

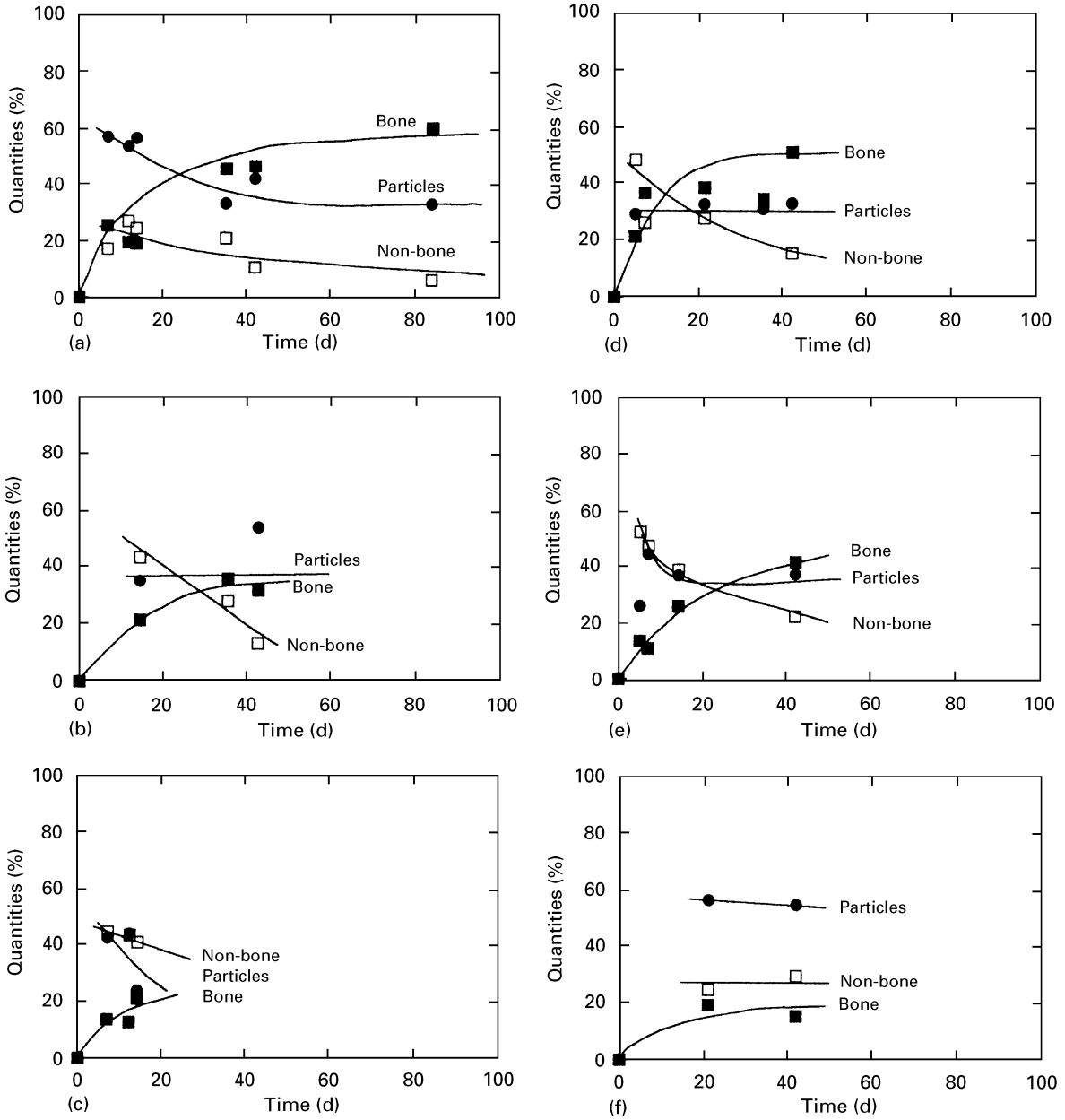

Figure 1 Percentages of regenerated bone regions, particles of Bioglass® and HA, and area of soft tissue in scanning electron micrographs (from [3, 4]), (a, c) at the periphery of the implantation site filled with Bioglass®. (a) ×400, (c) ×150; (b) at the centre of the implantation site filled with Bioglass®, ×400; (d, e) at the periphery of the implantation site filled with HA, (d) ×400, (e) ×150; (f) at the centre of the implantation site filled with HA, ×150. View areas: (a–c) 0.10 mm², (d–f) 0.90 mm².

3. Results

The percentages of Bioglass® and HA particles, area of soft tissue, and regenerated bone regions as a function of implantation time are shown in Fig. 1a–f. The average data of ×400, ×150, and ×60 micrographs are summarized in Table I. As shown in Fig. 1a, the rate of bone generation in the Bioglass® samples increased immediately with time, and then stabilized at around 6 wk. The percentages of regenerated bone regions were ~50%, and ~60% for 6 and 12 wk, respectively. The amount of Bioglass® particles and area of soft tissue decreased slowly at long implantation times. Soft tissue represented ~6% at 12 wk. The degree of bone generation similarly increased with time at the centre of the implantation site (shown in Fig. 1b). The amount of generated bone was smaller at the centre than at the periphery for all times.

These results show that new trabecular bone was rapidly generated at early times (between 1 and 6 wk) on the surface of Bioglass® particles. The interparticle spaces filled with new bone increased with implantation time from the periphery to the centre of the implantation site.

The effect of magnification on the analysis is shown in Fig. 1a and d. The percentage of bone regeneration observed in the image at ×150 is similar to that of ×400, but the area of non-bone is larger at early times for ×150 observation. The new bone was ~37% and ~52% for 1 and 6 wk, respectively, for ×150 observation. The distribution of bone in high-magnification images is larger than that in low-magnification images, as there is a decrease in the amounts of particle, soft tissue, and generated bone. However, these two magnification

TABLE I Point-counting percentage of regenerated bones, particles of 45S5 Bioglass®, and area of soft tissue in scanning electron micrographs [3, 4] by hand-point-counting technique at various implantation times

Materials	Location of implantation site	Time (d)	Percentage of point-counting (%)			
			Particles	Soft tissue	Original bone	Regenerated bone
Bioglass®	Periphery	5	30.6 ± 0.9	46.0 ± 2.7	6.6	16.8 ± 4.9
		7	47.0 ± 9.9	21.8 ± 4.5	0.0	31.2 ± 5.5
		12	40.9 ± 12.7	37.0 ± 10.1	8.7	13.4 ± 6.2
		14	56.4	24.6	0.0	19.0
		21	32.4 ± 0.5	29.3 ± 1.1	8.9	29.4 ± 9.6
		35	30.2 ± 5.2	31.7 ± 11.8	2.0	36.1 ± 12.7
		42	37.8 ± 4.6	11.5 ± 0.5	1.4	49.3 ± 2.5
		84	33.5	6.4	0.0	60.1
	Centre	14	45.3 ± 10.0	40.0 ± 3.5	0.0	14.7 ± 6.6
		21	54.1 ± 1.9	26.0 ± 1.1	0.0	20.0 ± 0.8
		35	41.6 ± 6.9	28.8 ± 2.0	0.0	29.6 ± 7.7
		42	51.6 ± 2.6	19.0 ± 5.3	0.0	29.4 ± 2.7
HA	Periphery	5	27.9 ± 2.3	54.7 ± 3.6	10.3	7.1 ± 6.4
		7	42.7 ± 0.5	45.2 ± 0.9	0.0	12.1 ± 1.4
		12	43.5	43.2	0.8	12.5
		14	32.3 ± 10.2	34.6 ± 11.9	11.9	21.2 ± 6.0
		21	34.9	33.3	13.6	18.2
		42	27.1 ± 10.7	24.9 ± 2.3	18.3	29.7 ± 11.4
		84	38.3	40.8	5.1	15.8
	Centre	14	51.7	40.8	0.0	7.5
		21	44.4	32.0	0.0	23.6
		42	56.1 ± 1.3	28.6 ± 1.0	0.0	15.3 ± 0.3
		84	49.4	33.7	0.0	16.8

images produce similar results in amount of regenerated bone.

As shown in Fig. 1e and d, the percentage of regenerated bone regions at the periphery of the hole for implanted HA particles increased slowly with time, while the area of soft tissue gradually decreased. The rate of bone regeneration on the HA particles was clearly slow, as compared with that of Bioglass® (shown in Fig. 1d) at the periphery of the implantation site for early times. The amounts of new trabecular bone were ~ 11% and ~ 41% for 1 and 6 wk, respectively. Furthermore, the rate of loss in the interparticle space filled with HA particles was slow as compared with Bioglass®. The amount of generated new bone was only ~ 16% at the centre by 6 wk for HA samples. Thick bone bridges between HA particles were not found, but a partial thin bone layer appeared on the surface of some HA particles.

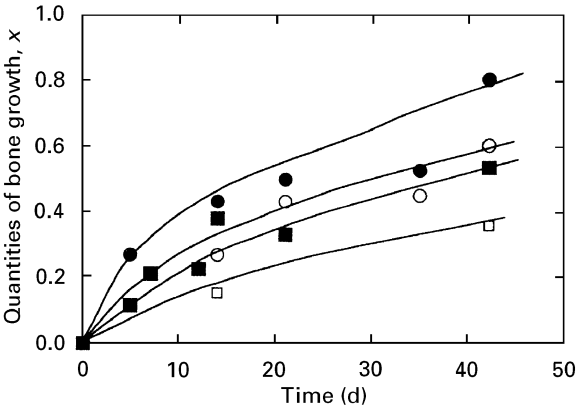

Figure 2 Relationship between ratio of bone growth and time as compared with materials and location of the implantation site: (●) 45S5 Bioglass (periphery), (○) 45S5 Bioglass (centre), (■) HA (periphery), (□) HA (centre).

4. Kinetic analysis

The time dependences of ratio of bone growth, x (see Equation 3), for Bioglass® and HA particles are plotted in Fig. 2, and the relationships between $1-(1-x)^{1/3}$ and time are shown in Fig. 3. As shown in Fig. 3, the formation of bone on the surface of Bioglass® and HA particles can be described by the surface chemical reaction-controlled shrinking core model expressed by

$$1-(1-x)^{1/3} = kt \quad (4)$$

where k is the rate constant of bone growth [7, 8] and t is the time. The rate constants of Bioglass® and HA at both the periphery and the centre of the femoral hole measured from the slope in Fig. 3, and bioactive index, I_B, measured from the experimental bone bonding reaction [9] are listed in Table II. The bioactive index is given by $I_B = (100/t_{0.5bb})$, where $t_{0.5bb}$ is the time for more than 50% of the surface to be bonded to bond [5].

The rate constants of bone growth for Bioglass® particles were $10.9 \times 10^{-3}\,d^{-1}$ at the periphery, and $7.2 \times 10^{-3}\,d^{-1}$ at the centre of the femoral hole. The rate constants of Bioglass® were larger than that of HA particles. Furthermore, these results show the higher bioactivity of Bioglass®, in agreement with the range of bioactive index I_B previously reported for

TABLE II Relationship between the rate constants of *in vivo* bone generation and the bioactive indices using particulate 45S5 Bioglass® and HA particles

Materials	Location of implantation site	Experimental rate constants[a] ($10^{-3}\,d^{-1}$)	Bioactivity bonding index, I_B[b] (d^{-1})
45S5 Bioglass®	Periphery	10.9	12.5
	Centre	7.2	
HA	Periphery	4.6	3.1
	Centre	2.0	

[a]Estimated from the surface chemical reaction-controlled shrinking-core model [7, 8].
[b]$I_B = 100/t_{1/2bb}$.

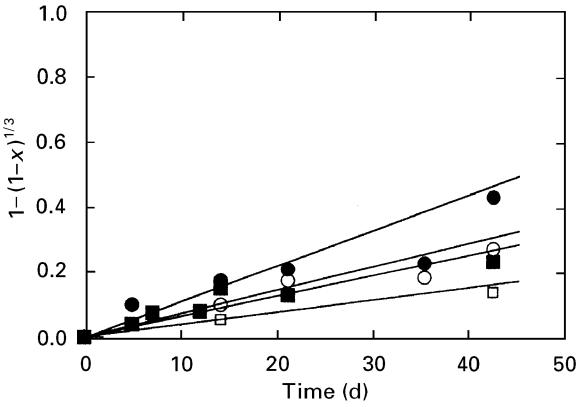

Figure 3 Plots of $1-(1-x)^{1/3}$ as a function of time: (●) 45S5 Bioglass (periphery), (○) 45S5 Bioglass (centre), (■) HA (periphery), (□) HA centre.

these materials [9]. The biochemical behaviour of Bioglass® and HA with respect to bone formation and bonding is greatly different, as discussed previously [10, 11]. The precise reasons for the difference in rate of bone growth are not clear. However, chemical differences in the surface of the materials may be important for generating new trabecular bone which involves differentiation and proliferation of bone cells [9]. The differences in osteogenic behaviour of Bioglass® and HA particulate were revealed by the difference in rate constants of bone regeneration measured in this rabbit femoral model.

5. Conclusions

1. The bone growth rate constants for Bioglass® were estimated to be $\sim 10.9\times10^{-3}\,d^{-1}$ at the periphery and $\sim 7.2\times10^{-3}\,d^{-1}$ at the centre of the implantation site using a hand-point-counting technique.

2. The rate constants for HA particles under similar *in vivo* conditions were $4.6\times10^{-3}\,d^{-1}$ at the periphery of implantation site and $2.0\times10^{-3}\,d^{-1}$ at the centre.

3. For Bioglass®, trabecular bone was generated by 1 wk, with $\sim 80\%$ interparticle spaces being filled with new bone at the periphery of the implantation site in less than 6 wk.

4. The rate of bone growth for HA particles was relatively slow; the percentage of new bone growth is $\sim 30\%$ at 6 wk.

5. The higher activity of particulate Bioglass® in terms of the rate of trabecular bone growth agrees well with previously established rate constants for bulk Bioglass® implants in cortical bone.

References

1. G. E. MERWIN, *Ann. Otol. Rhinol Laryngol.* **95** (1986) 78.
2. J. WILSON, E. DOUEK and K. RUST, *Bioceramics* **8** (1995) 239.
3. H. OONISHI, S. KUSHITANI, H. IWASAKI, K. SAKA, H. ONO, A. TAMURA, T. SUGIHARA, L. L. HENCH, J. WILSON and E. TSUJI, *ibid.* **8** (1995) 137.
4. H. OONISHI, S. KUSHITANI, E. YASUKAWA, H. KAWAKAMI, A. NAKATA, S. KOH, L. L. HENCH, J. WILSON and E. TSUJI and T. SUGIHARA, *ibid.* **7** (1994) 139.
5. L. L. HENCH and J. WILSON, "An Introduction to Bioceramics" (World Scientific, New York, 1993) p. 41.
6. L. L. HENCH and R. W. GOULD, "Characterization of Ceramics" (Marcel Dekker, New York, 1971) p. 529.
7. J. M. SMITH, "Chemical Engineering Kinetics", 3rd Edn (McGraw-Hill, New York, 1981) p. 642.
8. F. HABASHI, "Principles of extractive metallurgy", Vol. 1 (Gordon and Breach, New York, 1969) p. 121.
9. L. L. HENCH and J. K. WEST, *Life Chem. Rep.* **13** (1996) 187.
10. L. L. HENCH, *J. Am. Ceram. Soc.* **74** (1991) 1487.
11. M. JARCHO, *Clin. Orthop. Relat. Res.* **157** (1981) 259.

Received 30 September 1996
and accepted 6 March 1997